A projection selection method to improve image quality in optical projection tomography

Jin Guo[1#], Yujie Yang[2#], Di Dong[2], Liangliang Shi [2], Hui Hui[2], Min Xu[2], Jie Tian[2]-IEEE Fellow and Xia Liu[1]*

Abstract—**Optical projection tomography (OPT) is a very important imaging tool for a mesoscopic-scale. It can provide three dimensional (3D) transmission and emission imaging. However, high-resolution OPT is limited in depth of field (DOF) due to a high numerical aperture, which causes a poor performance of OPT in imaging large samples. Moreover, it is difficult to tune the focus plane (FP) to a fixed position where OPT always has the best image quality in different directions. To address these problems, we developed a projection selection method to improve DOF in OPT. In each direction, our method automatically selects the best projection from several projections with different FP. Then, we use a series of selected projections for 3D reconstruction. The experimental results demonstrate that our method can improve the image quality comparing to a fixed FP. Moreover, our method is flexible to be used in other OPT setups by adding a linear stage.**

I. INTRODUCTION

Optical projection tomography (OPT) is a technique that can realize highly specific and structural 3D imaging [1].It has many advantages such as high resolution, integration of structure and function, no radiation, low cost and so on. It can conduct qualitative and quantitative research at the cellular level for small scale animals, realizing real-time, noninvasive, dynamic and *in vivo* imaging. Currently, OPT technology has been applied to 3D imaging of gene and protein expression patterns in tissue specimens. OPT provides an effective tool for small specimens such as embryos, *Drosophila melanogaster* pupa and engineered tissue, promoting the development of biological science basic research. Recently, helical optical projection tomography has also been developed to view elongated samples [2].

Scattering effect can be neglected when visible light transmits through the sample, because the sample from OPT scanning has been rendered transparent by chemical clearing or is inherently transparent [3]. It is assumed that the light travels in straight lines through the samples, which mainly show the absorption of visible light. When acquiring the OPT image, mount the sample on a high precision rotation stage, use a high-stability LED or laser as the light source, so that the images will be acquired by a highly sensitive CCD at a fixed angle interval over a full rotation of the sample. The data acquired by OPT were a series of 2D projections, and these projections were reconstructed using a filtered back projection (FBP) algorithm [4]. The quality of 2D projections is related to the resolution of the 3D reconstruction. When the sample was rotated out of focus, reconstructed OPT images may suffer from blurring caused by rotational axis deviation or the error of the mechanical device. In any given optical image, the objects at the focal plane are in optimal focus, so the objects within the DOF are considered to be in focus and the objects outside the depth of field are considered to be out of focus [5].

In this paper, we present a method that acquires a series of projections by locating them in different FP at the same angle. Then, we automatically select the best quality projection from several projections to employ the selected projections to reconstruct the 3D image. The organization of the paper is as follows. In the next section, we show the experimental setup. In section III, we describe the method. In section IV, we analyze the performance of the projection selection method. In the last section, we discuss relevant issues.

II. OPT SYSTEM

Here we demonstrate our homebuilt OPT setup using the experimental configuration depicted in Figure 1. We collect the light transmitted through the sample using a 13.3mm×13.3mm imaging area Electron-Multiplying CCD (EMCCD) (iXonDU888, Andor, UK), which is an active pixel 1024 × 1024 imaging array and consists of a cooled temperature at -95ºC. The light travels through a modular objective lens system (Z16 APO, Leica, Germany), which creates a geometrically correct projection of the transmission in a plane perpendicular to its optical axis. The sample was mounted under a rotation stage (ANT95-360-R, Aerotech, USA) and suspended in a refractive-index matched environment (*ex vivo* tissue) or in the air (*in vivo* tissue). The rotation stage was fixed on the vertical linear stage (NRT100/M, Thorlabs, USA), which can move back and forth with high stability and accuracy to satisfy the requirements of the experiment. A commercial 488 nm laser (DL-488-050, CrystaLaser, USA) was used to provide continuous wave excitation and a diffuser to provide uniform illumination over the entire sample. The whole experiment was conducted in an

[1]Jin Guo and Xia Liu are with the School of Automation, Harbin University of Science and Technology, Harbin 150080, China.

[2]Yujie Yang, Di Dong, Liangliang Shi, Hui Hui, Min Xu and Jie Tian are with the Key Laboratory of Molecular Imaging, Institute of Automation, Chinese Academy of Sciences, Beijing 100190, China.

\# These authors have contributed equally to this work.

* Corresponding author, phone: 86451-86390157; Fax: 86451-86390157; email: liuxia@hrbust.edu.cn.

optical-isolated box and all the imaging devices were fixed on the optical platform. A control software has been developed based on the QT platform to process the experiment automatically. In the conventional experiment, we collect 400 2D images by rotating the sample with a rotation step of 0.9º along the vertical axis. However, as in the method shown in this paper, the projection quantity should be adapted to the size of the sample we mounted.
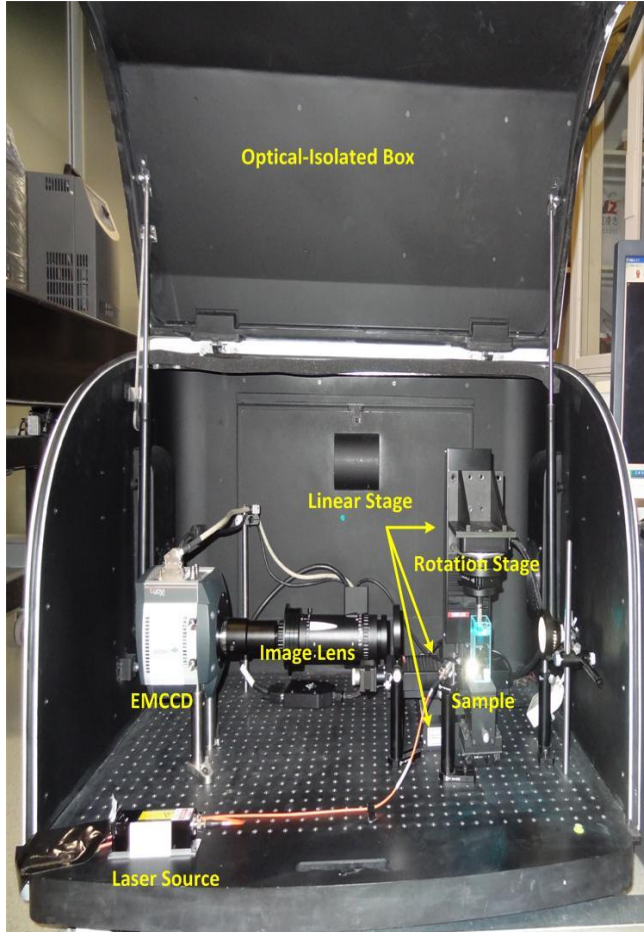

Figure 1.   Physical map for optical projection tomography setup. This setup is made of the image acquisition model, mechanical movement model, light source model and control model (*not in the picture*).

III.   METHOD

A. Imaging problems

As shown in Figure 2, for the rotational axis deviation and the error of the mechanical device, the sample may be rotated out of focus, leading to the blurred projection. As shown in Figure 3, the images are at two orthogonal angular projections. The image at 0° is blurred, but the image at 180° is clear. Namely, when acquiring data, some part of the specimen may be rotated outside the depth of field.

B. Image acquisition

In general, OPT projections were acquired by adjusting the position of the axis of the rotation so that only the front half of

the specimen was in focus [1]. As a result, some out-of-focus data from the half of the specimen outside the depth of field are super imposed on the in-focus data from within the depth of field. Then, these out-of-focus data are included in the FBP reconstruction process and could contribute to the lack of focus in the 3D image [5].
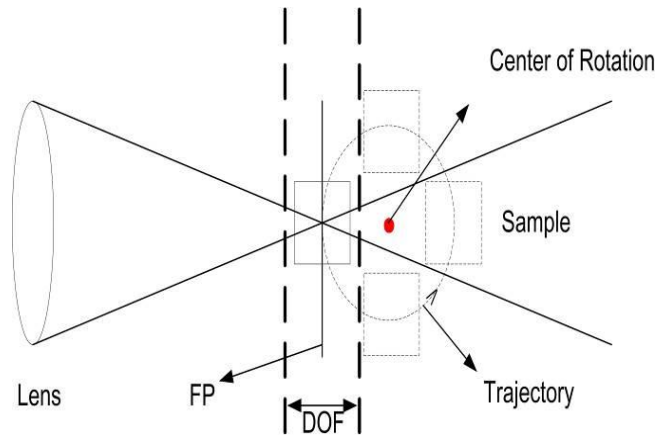

Figure 2.   Problem of sample rotated out of focus. DOF, depth of field; FP, focal plane. When acquiring data, the sample may be rotated out of focus, even if it was in the DOF.
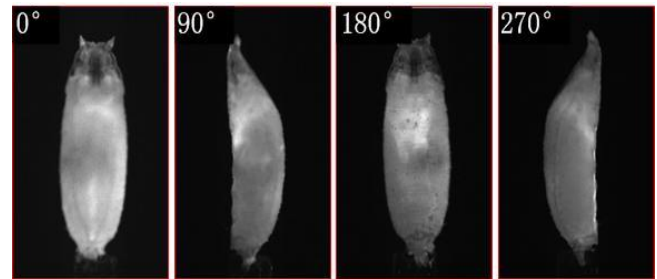

Figure 3.   Two orthogonal angular projections. When acquiring data, it is definite that some parts of the samples will be rotated out of focus.
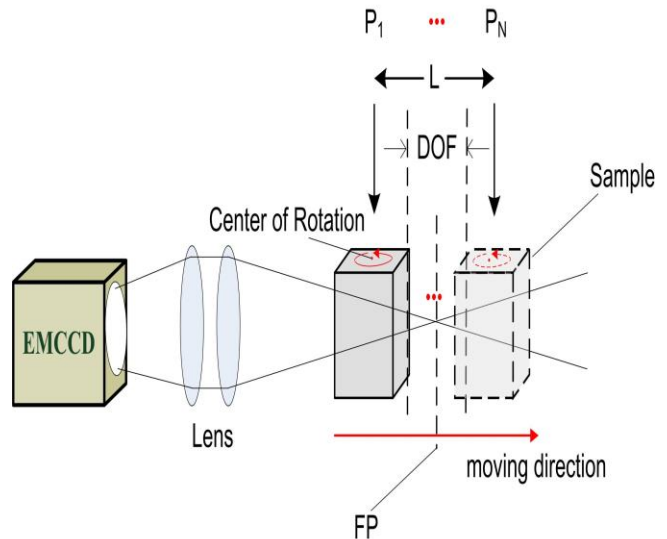

Figure 4.   Schematic of projection selection. DOF, depth of field; FP, focal plane; P, position; L, the distance between two boundaries; N, total steps. To get an optimal projection at one angle, we move the sample along the axis of EMCCD. It can avoid the sample rotation outside of the depth of field.

In this paper, as shown in Figure 4, our projection selection method is to move the linear stage along the axis of the EMCCD, while the projections acquired by EMCCD are changed from blurred to clear to blurred, because the samples show clear only in the FP. The two blurred projections are corresponding to the boundaries of the high quality projections, i.e. the optimal projection which is between two boundaries. The step pitch is calculated by

$$d = L/N \qquad (1)$$

where d is the step pitch, L is the distance between two boundaries and N is the total of steps. N is determined by the accuracy we need. If the demand of accuracy is high, the N should be increased. Then, we collect $N+1$ projections at one angle. Considered the imaging efficiency, we choose $N<10$. Generally, all clear projections in full rotation are covered in the L distance. Even though this method spends some more time than before, we can obtain high quality 3D image.

When the projections have been collected at one angle, the rotation stage rotates 0.9º to collect projections at the next angle. The image acquisition process will be stopped before the rotation stage rotates 360º, so the acquired projections are $400 \times (N+1)$.

C. Projection selection

As shown in Figure 5, there are a series of projections from blurred to clear to blurred. Out-of-focus data from the half of the specimen outside the depth of field are included in the FBP reconstruction process and would contribute to the lack of focus in the 3D image.
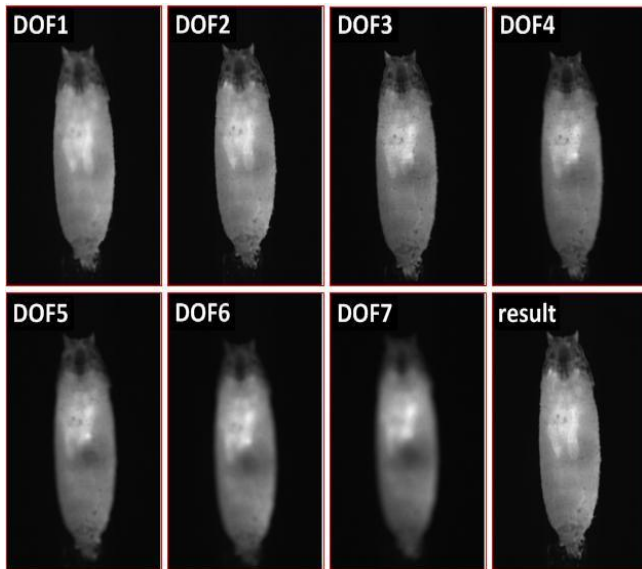

Figure 5.   Projection selection based on high frequency content calculations. From DOF1 to DOF7, the projection underwent from blurred to clear to blurred. Through our calculations, we obtaine the optimal projection as DOF2, so the result is DOF2.

We select the optimal projection at any angle, using high frequency content calculations. When the projection is blurred, the high spatial frequency content of the image decreased. Then, we can measure the high frequency content in the image

to decide which one to choose. It is calculated by the following function.

$$F^{1}_{n,m,\theta} = \iint\limits_{image} E\left\{ \left| \frac{\partial^{n} g(x,y)}{\partial x^{n}} \right| - \theta \right\}^{m} dxdy$$

$$(2)$$

Where $g(x, y)$ is the grey value at (x, y), θ is an arbitrary threshold and $E(z) = z$ if $z \geq 0$; $E(z) = 0$ if $z < 0$. In this function, the higher frequency components in the image are measured by differentiation of the image and summing the values over the image [6].

The projection selection is completed by the MATLAB process. In the projection selection process, we set one loop to process $N+1$ projections at one angle, and another to process full rotation projections. As a result, DOF2 is the optimal one.

IV.   RESULTS AND DISCUSSION

FBP algorithm is performed to reconstruct 3D imaging using these selected projections. The final format of 3D images is .raw. Then, we use 3DMed [7] for the analysis, which was developed by our group (http://www.3dmed.net/, http://www.mitk.net/). The results are shown in Figure 6. From the results, we could distinguish the salivary glands of *Drosophila melanogaster* pupae.
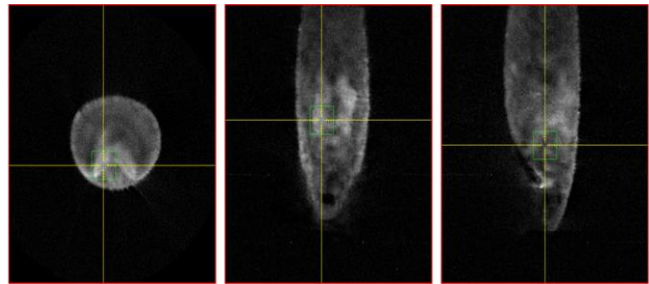

Figure 6.   Experimental result analysis of *Drosophila melanogaster* pupae. It clearly shows the transverse, sagittal and coronal views.

This approach is easy to realize, but the scattering is also remarkable for *Drosophila melanogaster* pupa research[8]. Because of the scattering, we cannot get the absolutely clearest sample projection at any location. In our future work, image fusion from a series of projections acquired by our method will be used to make a clear projection for 3D reconstruction.

V.   CONCLUSION

In this paper, we proposed a projection selection method to improve the image quality in OPT. In each angle, we acquired several projections with different FP positions and only the projection with the maximum high spatial frequency content was selected to be involved in the final reconstruction. Through this way, we found the sharpest image in each angle and these projections led to a high-resolution reconstruction. Although we only showed an emission experiment on *in vivo Drosophila melanogaster* pupae, our method can also be used in transmission OPT and other specimens. Furthermore, our

work leaves much room for improvement. Our method is a bit time-consuming since we acquired multiple projections in each direction. In the future, we will set a narrow FD search region to reduce the image acquisition time. Moreover, the selection step may lose some details in projections from the unselected FDs. In our further work, we will replace the selection step with a merging of different projections.

REFERENCES

[1] J. Sharpe, U. Ahlgren, P. Perry, B. Hill, A. Ross, J. Hecksher-Sorensen, R. Baldock, D. Davidson, "Optical projection tomography as a tool for 3D microscopy and gene expression studies," *Science*, vol. 296, pp. 541-545, 2002.

[2] A. Arranz, D. Dong, S.P.Zhu, M. Rudin, C. Tsatsanis, J. Tian, and J. Ripoll, "Helical optical projection tomography,"*Optics Express*, 21(22): 25912-25925, 2013.

[3] U. J. Birk, M. Rieckher, N. Konstantinides, A. Darrell, A. Sarasa-Renedo, H. Meyer, N. Tavernarakis, J. Ripoll, "Correction for specimen movement and rotation errors for in-vivo Optical Projection Tomography," *Biomed. Opt. Express* 1, 87, 2010.

[4] D. Dong, S.P. Zhu, C.H. Qin, V. Kumar, J.V. Stein, S. Oehler, C. Savakis, J. Tian, J. Ripoll, "Automated Recovery of the Center of Rotation in Optical Projection Tomography in the Presence of Scattering," *IEEE J Biomed Health*, vol. 17, pp. 198-204, 2013.

[5] J.R. Walls, J.G. Sled, J. Sharpe, R.M. Henkelman, "Resolution improvement in emission optical projection tomography," *Phys Med Biol*, vol. 52, pp. 2775-2790, 2007.

[6] Groen FCA, Young IT, Lighthart G, "A comparison of different focus functions for use in autofocus algorithms," *Cytometry*, 6: 81–91, 1985.

[7] J. Tian, J. Xue, Y.K. Dai, J. Chen, J. Zheng, "A Novel Software Platform for Medical Image Processing and Analyzing," *IEEE T Inf Technol B*, vol. 12, pp. 800-812, 2008.

[8] S.P. Zhu, D. Dong, U.J. Birk, M. Rieckher, N. Tavernarakis, X.C. Qu, J.M. Liang, J. Tian, J. Ripoll, "Automated Motion Correction for In Vivo Optical Projection Tomography," *IEEE T Med Imaging*, vol. 31, pp. 1358-1371, 2012.